Structure

Article

Structural Insights into the Molecular Recognition between Cerebral Cavernous Malformation 2 and Mitogen-Activated Protein Kinase Kinase Kinase 3

Graphical Abstract

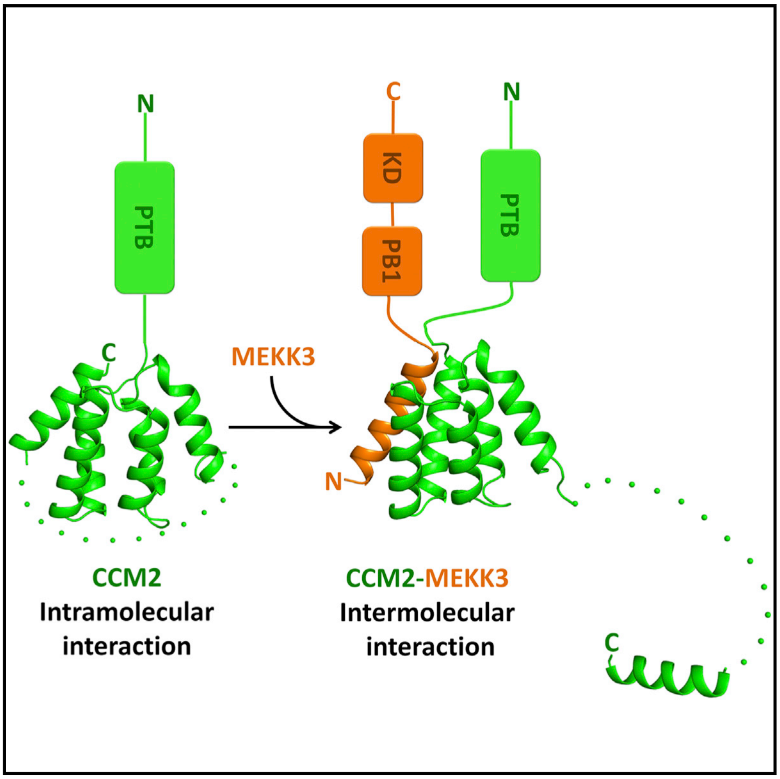

Authors

Xiaoyan Wang, Yanjie Hou, ...,
Da-Cheng Wang, Jingjin Ding

Correspondence

jding@moon.ibp.ac.cn (J.D.),
dcwang@ibp.ac.cn (D.-C.W.)

In Brief

CCM2 functions as an adaptor protein that mediates the activation of MEKK3 signaling in response to osmotic stress, or negatively regulates MEKK3 signaling, which is important for normal cardiovascular development. Wang et al. reveal the structural basis governing the molecular recognition between CCM2 and MEKK3.

Highlights

- CCM2ct assembles into a global six-helix domain by intramolecular interaction
- CCM2ct intramolecular interaction is weak
- MEKK3-n_{helix} is the crucial structural element for CCM2ct binding
- The binding of CCM2ct to MEKK3-n_{helix} resembles CCM2ct intramolecular interaction

Wang et al., 2015, Structure *23*, 1087–1096
June 2, 2015
http://dx.doi.org/10.1016/j.str.2015.04.003

Structural Insights into the Molecular Recognition between Cerebral Cavernous Malformation 2 and Mitogen-Activated Protein Kinase Kinase Kinase 3

Xiaoyan Wang,[1,2] Yanjie Hou,[1] Kai Deng,[1,3] Ying Zhang,[1] Da-Cheng Wang,[1,*] and Jingjin Ding[1,*]
[1]National Laboratory of Biomacromolecules, Institute of Biophysics, Chinese Academy of Sciences, Beijing 100101, People's Republic of China
[2]Department of Clinical Oncology, Taihe Hospital, Hubei University of Medicine, Hubei 442000, People's Republic of China
[3]Reproductive Medicine Center, Renmin Hospital, Hubei University of Medicine, Hubei 442000, People's Republic of China
*Correspondence: jding@moon.ibp.ac.cn (J.D.), dcwang@ibp.ac.cn (D.-C.W.)
http://dx.doi.org/10.1016/j.str.2015.04.003

SUMMARY

Cerebral cavernous malformation 2 (CCM2) functions as an adaptor protein implicated in various biological processes. By interacting with the mitogen-activated protein kinase MEKK3, CCM2 either mediates the activation of MEKK3 signaling in response to osmotic stress or negatively regulates MEKK3 signaling, which is important for normal cardiovascular development. However, the molecular basis governing CCM2-MEKK3 interaction is largely unknown. Here we report the crystal structure of the CCM2 C-terminal part (CCM2ct) containing both the five-helix domain (CCM2ct$_s$) and the following C-terminal tail. The end of the C-terminal tail forms an isolated helix, which interacts intramolecularly with CCM2ct$_s$. By biochemical studies we identified the N-terminal amphiphilic helix of MEKK3 (MEKK3-n$_{helix}$) as the essential structural element for CCM2ct binding. We further determined the crystal structure of CCM2ct$_s$-MEKK3-n$_{helix}$ complex, in which MEKK3-n$_{helix}$ binds to the same site of CCM2ct$_s$ for CCM2ct intramolecular interaction. These findings build a structural framework for understanding CCM2ct-MEKK3 molecular recognition.

INTRODUCTION

Adaptor proteins are an emerging group of proteins that function as essential components of cellular signal transduction involved in gene expression, protein synthesis and quality control, cell metabolism, intracellular trafficking, cytoskeleton maintenance and rearrangement, cellular membrane dynamics, stress and immune response (Good et al., 2011; Pan et al., 2012). In cellular signal cascades, adaptor proteins evolve unique protein-protein and protein-ligand interaction modules to recruit their binding partners (Bhattacharyya et al., 2006; Flynn, 2001). Exploring the structural basis for adaptor-partner recognition could provide in-depth understanding of the complicated functions of related signal pathways in the cell.

Cerebral cavernous malformation 2 (CCM2) was initially characterized as a critical adaptor protein for mitogen-activated protein kinase (MAPK) cascade in response to osmotic stress. By bridging the upstream kinases MAPK/ERK kinase kinase 3 (MEKK3) and MAPK/ERK kinase 3 (MEK3) in the p38 MAPK phospho-relay pathway, CCM2 mediates the phosphorylation and ensuing activation of MEK3 by MEKK3, in turn activating downstream p38 MAPK and regulating cytoskeletal architecture (Uhlik et al., 2003). The gene encoding CCM2 has been identified as the second CCM-related gene (Denier et al., 2004; Liquori et al., 2003, 2007). Loss-of-function mutations in CCM2 result in human cerebral cavernous malformation, a common vascular lesion of the CNS that leads to headaches, seizures, stroke, and intracranial hemorrhage (Labauge et al., 2007). By physically interacting with the first CCM-related gene product KRIT1 (Krev1/Rap1A Interaction Trapped 1, also known as CCM1), CCM2 is coupled to transmembrane receptor heart of glass 1 (HEG1) signaling, which regulates the endothelial cell junction and maintains the vessel integrity (Kleaveland et al., 2009) and is involved in the signal pathway that inhibits small GTPase RhoA and its effector Rho kinase, consequently limiting actin stress fibers and vascular permeability (Borikova et al., 2010; Crose et al., 2009; Stockton et al., 2010; Whitehead et al., 2009). Moreover, CCM2 can organize a large CCM signal complex via association with both Kirt1 and the third CCM-related gene product PDCD10 (programmed cell death 10, also known as CCM3) (Faurobert and Albiges-Rizo, 2010; Hilder et al., 2007; Voss et al., 2007; Zawistowski et al., 2005), which regulates vascular stability and growth dynamically (Rosen et al., 2013; Zheng et al., 2012). Full-length human CCM2 comprises 444 residues and adopts a two-domain architecture. The N-terminal part of CCM2 contains a canonical phosphotyrosine-binding (PTB) domain, which recognizes the NPxY/F (where x is any residue) motifs of Krit1 to perform related physiological functions (Hilder et al., 2007; Zawistowski et al., 2005). In neuroblastoma or medulloblastoma cells, the N-terminal PTB domain of CCM2 has been shown to interact with the juxtamembrane region of receptor tyrosine kinase TrkA, and the C-terminal part of CCM2 links to cell death by an unknown mechanism (Harel et al., 2009). Further studies indicated that germinal center kinase class III kinase STK25 is part of TrkA-CCM2-dependent death in medulloblastoma cells through CCM2-CCM3-STK25 interactions (Costa et al., 2012).

Table 1. Data Collection and Refinement Statistics

	CCM2ct	CCM2ct$_s$	CCM2ct$_s$-MEKK3-n$_{helix}$
Data Collection			
Space group	I4$_1$22	P6$_1$22	P4$_3$2$_1$2
Cell dimensions			
a, b, c (Å)	*a* = *b* = 113.30, *c* = 102.55	*a* = *b* = 51.36, *c* = 137.01	*a* = *b* = 61.21, *c* = 68.98
α, β, γ (°)	α = β = γ = 90.00	α = β = 90.00, γ = 120.00	α = β = γ = 90.00
Wavelength (Å)	0.97916	0.97908	1.54180
Resolution (Å)	45.41–2.70 (2.85–2.70)	37.31–1.93 (2.04–1.93)	45.78–2.10 (2.21–2.10)
Unique reflections	9,435 (1,351)	8,320 (1,170)	8,073 (1,092)
R_{merge} (%)	7.7 (38.1)	4.2 (7.9)	5.5 (29.8)
Average $I/\sigma(I)$	23.1 (6.9)	55.5 (30.5)	31.2 (5.9)
Completeness (%)	99.7 (100.0)	97.3 (96.7)	99.4 (96.4)
Redundancy	14.3 (14.7)	21.1 (21.8)	11.0 (6.8)
Refinement			
Resolution (Å)	43.19–2.70 (3.09–2.70)	31.86–1.93 (2.21–1.93)	45.78–2.10 (2.40–2.10)
No. of reflections	9,422 (3,081)	8,320 (2,671)	8,036 (2,565)
R_{work}/R_{free} (%)[a]	21.90/26.67 (29.61/35.71)	20.04/23.46 (21.77/29.53)	20.33/23.72 (20.64/27.02)
No. of atoms			
Protein	844	688	858
Water	0	74	70
B factors (Å^2)			
Protein	67.36	26.11	29.30
Water	0	36.37	35.58
Root-mean-square deviations			
Bond lengths (Å)	0.004	0.014	0.002
Bond angles (°)	0.701	1.406	0.636
Dihedral angles (°)	14.800	14.792	13.001
Chirality (°)	0.045	0.087	0.040
Planarity (Å)	0.002	0.007	0.002
Ramachandran plot			
Favored (%)	100.0	100.0	100.0

Values in parentheses represent the highest-resolution shell.
[a]5% of reflections are randomly selected for calculating R_{free}.

Although great efforts have been made to characterize the physiological functions of CCM2, the structural basis for the functional performance of CCM2, especially for that of its C-terminal part (CCM2ct), remains obscure. Recently, the structure of a truncated CCM2ct fragment (residues 283–379) was reported to be a five-helix compact domain (Fisher et al., 2013). This finding provides the preliminary structural information for CCM2ct, although the physiological significance of this structural feature has not been uncovered. Since initial characterization of CCM2-MEKK3 interaction in hyperosmotic stress signaling, further studies confirmed that CCM2-MEKK3 interaction is crucial for the activation of osmoprotective transcription factor via not p38 MAPK but phospholipase C-γ1 (Zhou et al., 2011). Later, CCM2-MEKK3 interaction was found to be associated with an Arp2/3 defect-induced non-autonomous effect on chemotactic signaling through the activation of nuclear factor κB downstream (Wu et al., 2013). Most recently, CCM2-MEKK3 interaction has been demonstrated to play an important role in endothelial cells for normal cardiovascular development. This interaction arrests MEKK3 in the CCM signal complex and inhibits MEKK3 signaling by negatively regulating endocardial expression of KLF2/4 transcription factors and ADAMTS4/5 proteases that degrade cardiac jelly (Zhou et al., 2015). This finding reveals a molecular mechanism by which CCM2-MEKK3 interaction functions in cardiovascular development that may also underlie CCM formation. However, the molecular basis governing CCM2-MEKK3 interaction remains largely unknown. Here, we present the crystal structure of CCM2ct, the biochemical studies that identify CCM2ct-MEKK3 recognition, and the complex structure of CCM2ct with an internal helix of MEKK3. Together, these findings reveal the structural basis for the molecular recognition between CCM2ct and MEKK3, and expand our knowledge on the action mode of the important adaptor protein CCM2.

RESULTS

Overall Structure of CCM2ct

Although the biological functions of CCM2 imply that it adopts a two-domain architecture, the structural and functional significance of CCM2ct could not be uncovered by sequence analysis. We successfully expressed, purified, and crystallized human CCM2ct comprising C-terminal residues beyond 289 (residues 290–444). The crystal structure of CCM2ct was determined by selenium single-wavelength anomalous diffraction at 2.70-Å in space group I4$_1$22 (Table 1). There is one CCM2ct molecule per asymmetric unit. Overall, CCM2ct assembles into a global six-helix domain, which contains both the truncated fragment as reported previously (named CCM2ct$_s$) and the following C-terminal tail. CCM2ct$_s$ consists of the tandem helices α1–α5 (residues 290–376), whereas the end of the C-terminal tail forms the isolated α6 helix (residues 421–436) (named CCM2-c$_{helix}$) (Figure 1A). The long loop (residues 377–420) connecting CCM2ct$_s$ and CCM2-c$_{helix}$, and the remaining residues beyond α6, are omitted in the final model due to the lack of interpretable electron density, indicative of their high intrinsic flexibility. In CCM2ct$_s$, the α1/α2 and α3/α4 helix pairs form two V-shape helix hairpins, bundling side by side to form the structural core of CCM2ct. The following α5 and α6 flank the clefts of α3/α4 and α1/α2 hairpins, respectively (Figure 1A). Sequence alignments among the CCM2ct homologs from different vertebrates also present high conservation of both parts of CCM2ct, but less sequence homology of the connecting loop (Figure 1B). This observation indicates that the structural feature we found in human CCM2ct is characteristic of all CCM2 homologs.

Intramolecular Interaction of CCM2ct

Structural homology searches using the Dali server (Holm and Sander, 1995) reveal that the structure of CCM2ct closely resembles that of the complex between the N-terminal domain of the Usher syndrome master scaffolding protein harmonin (named harmonin-nt) and an internal helix of cadherin23 (named

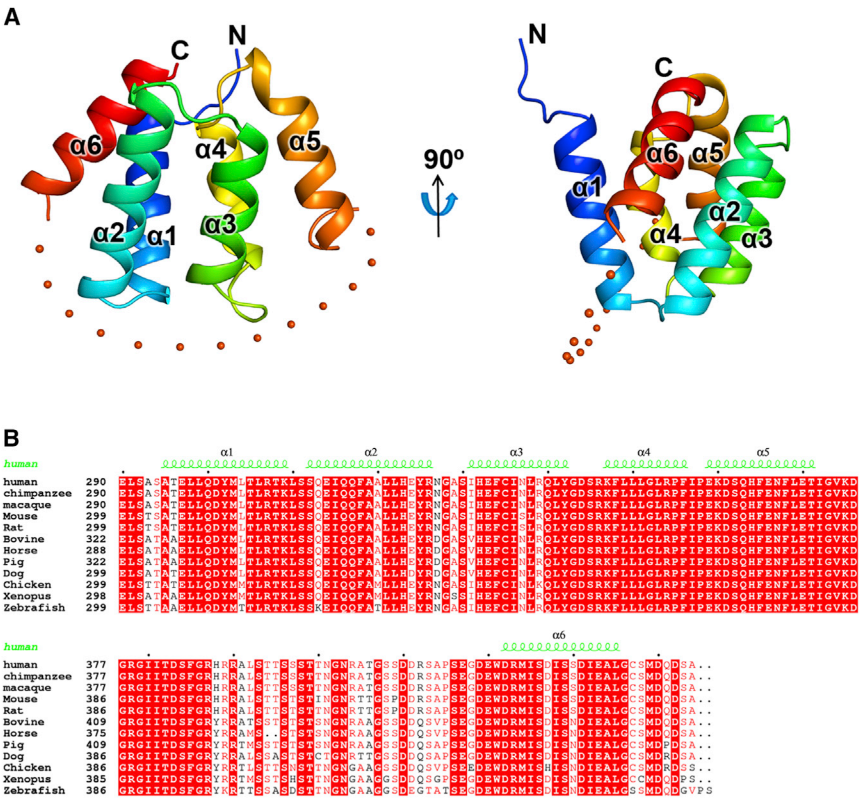

Figure 1. Structural Overview of CCM2ct

(A) Overall structure of CCM2ct in cartoon scheme as viewed from the front (left) and the side (right). Secondary structure elements are labeled. The long loop connecting CCM2ct$_s$ and CCM2-c$_{helix}$ is shown as a dotted line.

(B) Sequence alignment among the CCM2ct homologs from different vertebrates. Strictly conserved residues are highlighted with a red background. Similar residues are colored in light red. Secondary structures of human CCM2ct are schematically represented above the sequences.

cadherin23$_{helix}$), giving a Z score of 10.2. Superimposing the structure of CCM2ct on that of harmonin-nt-cadherin23$_{helix}$ complex yields a root-mean-square deviation of 2.0 Å for 78 Cα atoms and shows that CCM2ct$_s$ and CCM2-c$_{helix}$ are well aligned onto harmonin-nt and cadherin23$_{helix}$, respectively (Figure 2A). In the structure of harmonin-nt-cadherin23$_{helix}$ complex, the α1/α2 hairpin of harmonin-nt preforms a hydrophobic cleft to accommodate cadherin23$_{helix}$, resulting in tight binding between the two proteins (Pan et al., 2009). Both structural superimposition and structure-based sequence alignment indicate that the residues forming the α1/α2 V-shaped hydrophobic cleft of CCM2ct$_s$ are highly conserved with those of harmonin-nt (Figure 2B; Figure S1). Similar to cadherin23$_{helix}$ in the complex, CCM2-c$_{helix}$ is folded into a typical amphiphilic helix, with the hydrophobic face (composed of residues Met424, Ile425, Ile428, Ile432, and Leu435) embedded into the α1/α2 hydrophobic cleft of CCM2ct$_s$ (Figure 2C). In addition, Asp431 in CCM2-c$_{helix}$ forms two hydrogen bonds with the side chains of His323 and Arg326 in α2, serving as the supplement of CCM2ct$_s$-CCM2-c$_{helix}$ interactions (Figure 2C). These structural observations suggest that CCM2ct intramolecular interaction between CCM2ct$_s$ and CCM2-c$_{helix}$ is analogous to harmonin-nt-cadherin23$_{helix}$ binding. To verify that the major fragment CCM2ct$_s$ is a stable structural module like harmonin-nt, we also constructed, expressed, and crystallized CCM2ct$_s$ (Table 1). The solved structure of CCM2ct$_s$ is highly similar to that of harmonin-nt, consistent with the observation of a previous report (Fisher et al., 2013). Upon superimposing the structures of CCM2ct$_s$ and CCM2ct, CCM2ct$_s$ overlaps well with its counterpart in CCM2ct except for a slight deviation of the α1/α2 V-shaped cleft (Figure 2D). In the structure of CCM2ct, the α1/α2 angle is about 42° and the side chain of Arg326 takes a frizzy conformation to accommodate CCM2-c$_{helix.}$ However, in the structure of CCM2ct$_s$, the α1/α2 angle decreases to 32° and the side chain of Arg326 changes to an extended conformation, covering the α1/α2 cleft (Figure 2E). To investigate whether the intramolecular interaction observed in the structure of CCM2ct is metastable in solution, a CCM2 peptide (residues 417–438) containing CCM2-c$_{helix}$ was synthetized, and its binding affinity to CCM2ct$_s$ was measured by isothermal titration calorimetry (ITC) assay (Figure 3A). Data fitting yields a dissociation constant (K_d) of 82.0 μM between CCM2ct$_s$ and CCM2 peptide, suggesting that the CCM2ct$_s$-CCM2-c$_{helix}$ intramolecular interaction is weak. Binding of CCM2 peptide to CCM2ct was not detected by ITC measurement (Figure 3B). This result indicates that CCM2ct intramolecular interaction plays a competitive role in recruiting other targets. Next, the molecular mass of CCM2ct in solution was determined by analytical ultracentrifugation. The result shows a dominant peak with mean value of 17,859 ± 761 Da, which is very close to theoretical 18,463 Da of CCM2ct, demonstrating the monomeric state of CCM2ct in solution (Figure 3C). This observation implies that CCM2ct does not form stable dimers or oligomers by mutual interaction between CCM2ct$_s$ and CCM2-c$_{helix}$, which also suggests that CCM2ct intramolecular interaction is weak.

CCM2ct Directly Interacts with MEKK3 N-Terminal Helix

The striking structural similarity between CCM2ct and harmonin-nt-cadherin23$_{helix}$ complex, in addition to the weak CCM2ct intramolecular interaction, prompt the speculation that the α1/α2 hydrophobic cleft of CCM2ct could act as a potential binding site for CCM2 partner recruitment. The initial characterization of CCM2 showed that CCM2ct is the direct target of MEKK3 (Uhlik et al., 2003). Sequence and secondary structure analyses reveal that MEKK3 contains an isolated helix at its N terminus (residues 3–17, named MEKK3-n$_{helix}$), closely resembling the CCM2-c$_{helix}$ (Figure 4A). To determine whether MEKK3-n$_{helix}$ is directly recognized by CCM2ct, a MEKK3 peptide (residues 1–22) comprising MEKK3-n$_{helix}$ was synthesized, and its binding affinity to CCM2ct and CCM2ct$_s$ measured by surface plasmon resonance (SPR) experiments (Figure 4B). The K_d between

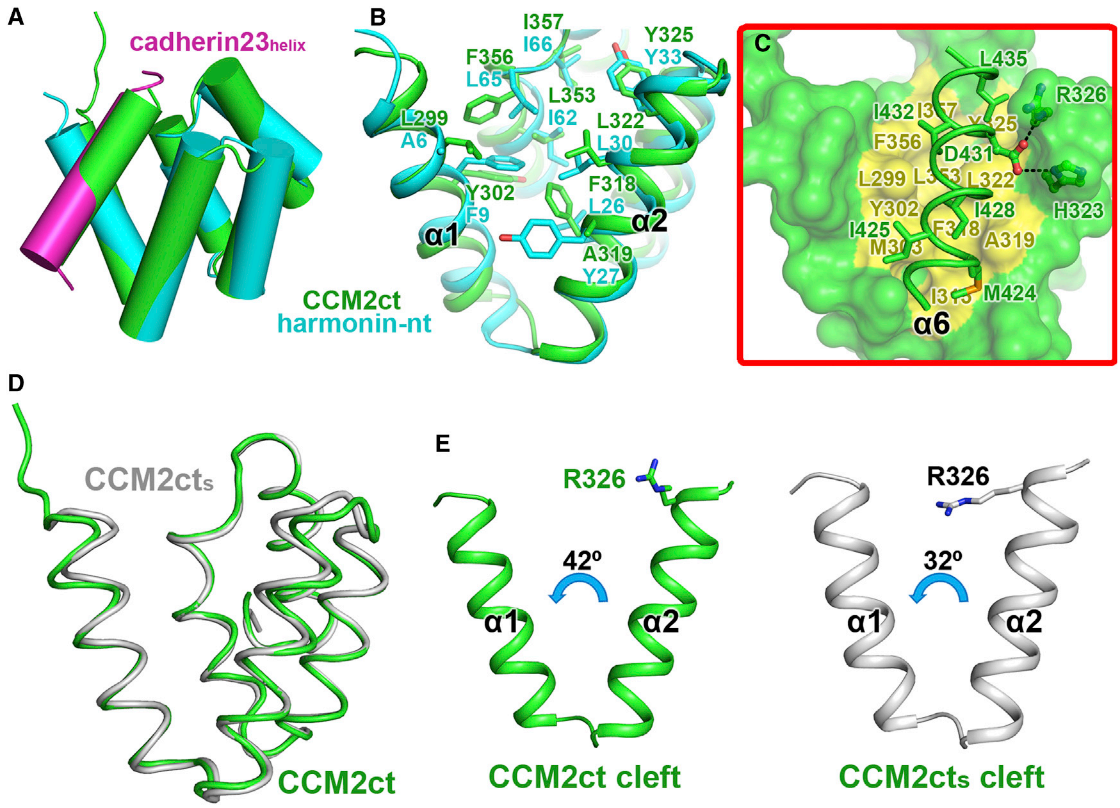

Figure 2. Intramolecular Interaction of CCM2ct

See also Figure S1.

(A) Structural superimposition of CCM2ct and harmonin-nt-cadherin23$_{helix}$ complex.

(B) Structural superimposition of CCM2ct$_s$ and harmonin-nt. The conserved hydrophobic residues forming the α1/α2 cleft of CCM2ct$_s$ and their counterparts in harmonin-nt are shown as stick models.

(C) Close-up view of the intramolecular interaction of CCM2ct. CCM2ct$_s$ and CCM2-c$_{helix}$ are represented as surface and ribbon models, respectively. The hydrophobic residues forming the α1/α2 cleft are labeled and colored yellow. The hydrophobic residues on CCM2-c$_{helix}$ are labeled and shown as stick models. Hydrogen bonds are shown as black dashes, and the involved residues are also shown as ball-and-stick models.

(D) Structural superimposition of isolated CCM2ct$_s$ and its counterpart in CCM2ct.

(E) Structural scheme of the variability of α1/α2 cleft and conformational change of Arg326.

MEKK3 peptide and CCM2ct or CCM2ct$_s$ are 9.59 and 3.25 μM, respectively, an order of magnitude lower than that of CCM2ct intramolecular interaction, which indicates that both CCM2ct and CCM2ct$_s$ were able to tightly bind to MEKK3-n$_{helix}$ due to the much higher affinity of the binding site to MEKK3-n$_{helix}$ than to CCM2-c$_{helix}$. To further confirm that MEKK3-n$_{helix}$ is the crucial structural element for CCM2ct-MEKK3 recognition in a protein context, two N-terminal fragments of MEKK3 were constructed and expressed. One comprises residues 1–126 (named MEKK3nt), including MEKK3-n$_{helix}$, the MEKK3 N-terminal Phox and Bem1p (PB1) domain, and the connecting loop. The other consists of residues 42–126, only containing MEKK3 N-terminal PB1 domain (named MEKK3nt$_s$). Ni pull-down assays indicate that both CCM2ct and CCM2ct$_s$ arrest MEKK3nt but not MEKK3nt$_s$ in vitro (Figure S2). In accordance with pull-down results, the binding affinities between MEKK3nt and CCM2ct or CCM2ct$_s$ can be determined by SPR measurements, whereas those between MEKK3nt$_s$ and CCM2ct or CCM2ct$_s$ are not detectable (Figure 4C; Figure S3). The K_d between CCM2ct$_s$ and MEKK3nt is only 7-fold lower than that between CCM2ct and MEKK3nt (Table 2), implying that the competitive role of CCM2-c$_{helix}$ in CCM2ct-MEKK3 intermolecular interaction is limited. These observations further confirm that CCM2ct intramolecular interaction is weak compared with CCM2ct-MEKK3 intermolecular interaction.

Structural Determinants Governing CCM2ct-MEKK3 Recognition

To explore the structural basis for CCM2ct-MEKK3 recognition, we determined the crystal structure of CCM2ct$_s$-MEKK3-n$_{helix}$ complex by co-crystallization. The complex structure was solved at 2.10-Å resolution by molecular replacement using the structure of CCM2ct$_s$ as model (Table 1). The unambiguous electron density helped us build the MEKK3-n$_{helix}$ model precisely (Figure S4). Each asymmetric unit contains one CCM2ct$_s$-MEKK3-n$_{helix}$ complex. The overall structure of the complex is highly similar to that of CCM2ct (Figure 5A). MEKK3-n$_{helix}$ adopts an amphiphilically helical conformation and binds into the α1/α2 hydrophobic cleft of CCM2ct$_s$. Residues Leu7, Ile10, Leu14, and Leu17 on the hydrophobic face of MEKK3-n$_{helix}$ flank the

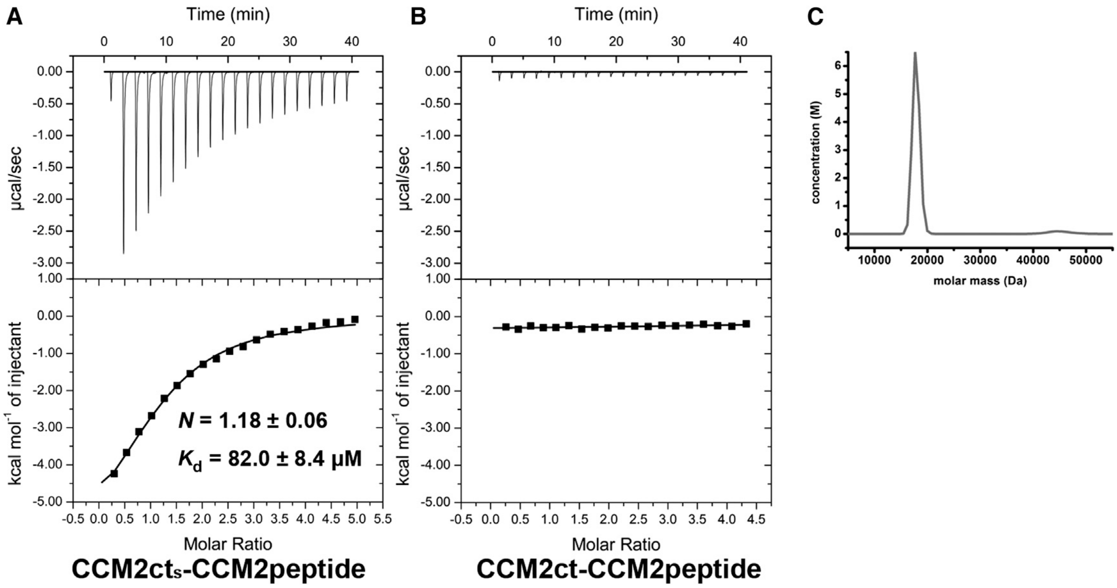

Figure 3. Biochemical Characterization of CCM2ct Intramolecular Interaction

(A) Profile of the titration of CCM2ct$_s$ to synthetized CCM2 peptide as measured by ITC. The binding parameters are indicated.

(B) Profile of the titration of CCM2ct to synthesized CCM2 peptide as measured by ITC.

(C) The molar mass profile of CCM2ct as determined by analytical ultracentrifugation.

hydrophobic cluster in the $\alpha1/\alpha2$ cleft of CCM2ct$_s$, similarly to their counterparts of CCM2-c$_{helix}$ in CCM2ct intramolecular interaction (Figure 5B). In addition, the conserved Asp13, corresponding to Asp431 of CCM2-c$_{helix}$, forms hydrogen-bond interactions with His323 and Arg326 of $\alpha2$ similar to those in CCM2ct intramolecular interaction (Figure 5B). From a structural viewpoint, CCM2ct employs the $\alpha1/\alpha2$ cleft to recruit MEKK3-n$_{helix}$ in the manner analogous to CCM2ct intramolecular interaction. The variability of the $\alpha1/\alpha2$ cleft is also observed in the CCM2ct$_s$-MEKK3-n$_{helix}$ complex. When superimposing the CCM2ct$_s$ in the complex with its counterpart in CCM2ct, the main deviation occurs in the $\alpha1/\alpha2$ cleft. The $\alpha1/\alpha2$ angle of CCM2ct$_s$ enlarges more for accepting MEKK3-n$_{helix}$ than for accommodating CCM2-c$_{helix}$ (Figure 5C). As a result, MEKK3-n$_{helix}$ is embedded deeper into the $\alpha1/\alpha2$ cleft than the CCM2-c$_{helix}$, contributing to closer hydrophobic contact (Figure 5D). In-depth inspection reveals that the non-conserved residues at both termini of MEKK3-n$_{helix}$ form extensive interactions with the $\alpha1/\alpha2$ cleft of CCM2ct$_s$, conferring the specific recognition between CCM2ct$_s$ and MEKK3-n$_{helix}$. At the N terminus, the long side chains of Trp421 and Met424 of CCM2-c$_{helix}$ hinder the insertion of conserved Ile425 and distance the N terminus of CCM2-c$_{helix}$ from the $\alpha1/\alpha2$ turn. However, Glu3 in MEKK3-n$_{helix}$, corresponding to Trp421 in CCM2-c$_{helix}$, interacts with Ser312 of the $\alpha1/\alpha2$ turn by a hydrogen bond, and Ala6 in MEKK3-n$_{helix}$ substitutes Met424 in the CCM2-c$_{helix}$. Both residue variations ablate the steric hindrance, and render the Leu7 of MEKK3-n$_{helix}$ (corresponding to Ile425 in CCM2-c$_{helix}$) embedded into the $\alpha1/\alpha2$ cleft and clamped by the aliphatic portion of the side chain of Arg307 in $\alpha1$ and hydrophobic Ile315 in $\alpha2$ (Figure 5E). At the C terminus, Three non-conserved hydrophobic residues of MEKK3-n$_{helix}$, Met11, Val15, and Met19, contribute additional hydrophobic interactions with Leu291 in the preceding N-terminal loop and Leu299 in $\alpha1$ of CCM2ct$_s$, generating a round of extension of $\alpha1$ at the N terminus (Figure 5F). Point mutations on the residues involved in the CCM2ct-MEKK3-n$_{helix}$ intermolecular interaction further confirm the structural determinants governing CCM2ct-MEKK3 recognition. On mutating either of the four crucial hydrophobic residues (Leu7, Ile10, Leu14, and Leu17) to charged Asp or substituting the conserved Asp13 to Ala in MEKK3, the binding between CCM2ct and MEKK3nt was completely abolished (Table 2), suggesting their determinative roles in CCM2ct-MEKK3 recognition. Mutation of the non-conserved Glu3 of MEKK3 to Ala induced only 2-fold reduction of the binding affinity between CCM2ct and MEKK3nt, indicating its auxiliary roles in CCM2ct-MEKK3 recognition (Table 2).

DISCUSSION

In this work, we discovered that CCM2 contains a well-folded adaptor domain at its C terminus. Although CCM2ct exhibits considerable structural homology with the N-terminal protein–protein interaction domain of the Usher syndrome master scaffolding protein harmonin, it presents unique structural features different from harmonin-nt. CCM2ct comprises both the structural module CCM2ct$_s$ corresponding to harmonin-nt, and the C-terminal structural element corresponding to the binding target of harmonin-nt. The two parts of CCM2ct could assemble into an integrated domain by intramolecular interaction analogous to the mechanism by which harmonin-nt binds to its target, a short internal helix of cadherin23. However, unlike the intermolecular interaction between harmonin-nt and cadherin23, which is strong and metastable, CCM2ct intramolecular interaction is weak. These structural distinctions between CCM2ct and harmonin-nt are functionally relevant. As the master scaffold protein of Usher protein complexes, harmonin interacts with cadherin23 firmly,

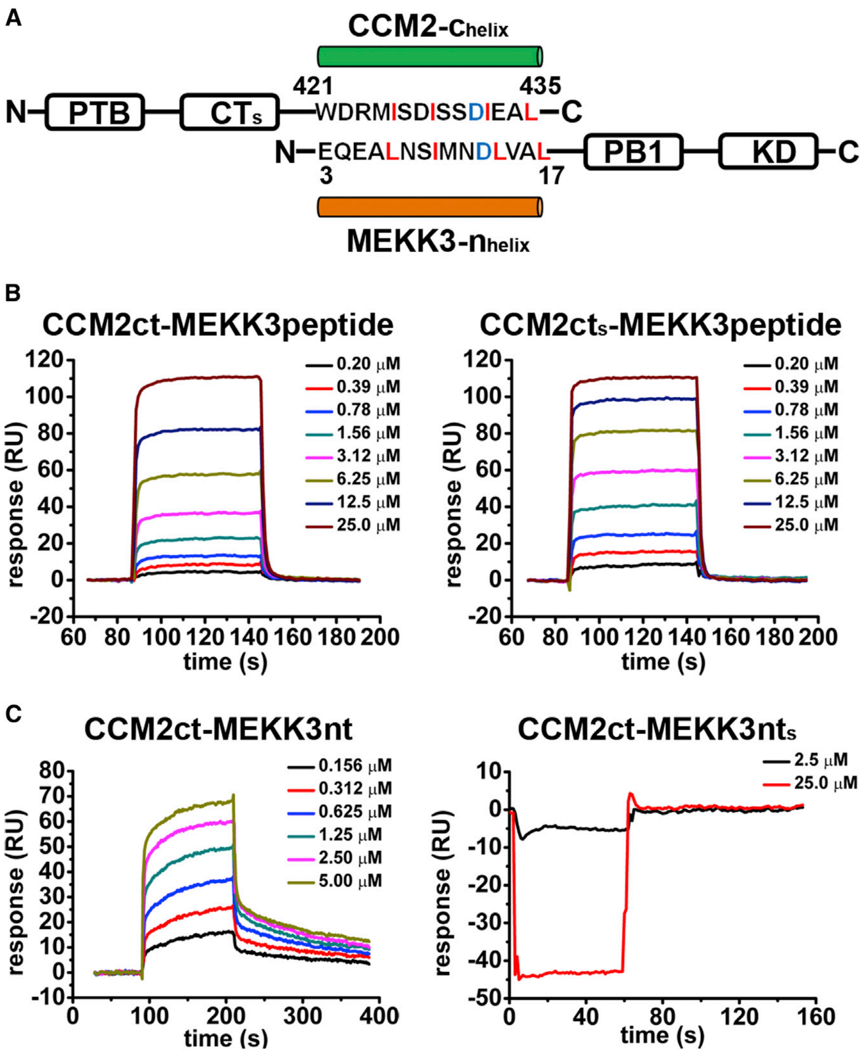

Figure 4. CCM2ct-MEKK3 Intermolecular Interaction

See also Figures S2 and S3.

(A) Domain schematic diagram of CCM2 and MEKK3 along with the sequence alignment of CCM2-c_{helix} and MEKK3-n_{helix}. The conserved residues in both helices are highlighted. PTB, phosphotyrosine-binding domain; PB1, Phox and Bem1p domain; KD, kinase domain.

(B) SPR sensorgram indicating the titrations of CCM2ct and CCM2ct_s by synthesized MEKK3 peptide at different concentrations.

(C) SPR sensorgram indicating the titrations of CCM2ct by MEKK3nt and MEKK3nt_s at different concentrations.

governing the functional tip links of hair cells (Pan et al., 2009). Therefore the binding site of harmonin-nt for cadherin23$_{helix}$ is pre-formed and unoccupied, and breaking this interaction causes dysfunction. CCM2 is an adaptor protein. Protein-protein interactions between CCM2 and its partners respond to diverse physiological conditions and are achieved precisely in time and space. This requires CCM2 to be able to switch between the resting state and the acting state, similarly to other adaptor proteins. Hence, in its resting state CCM2 evolves CCM2-c_{helix}, which could occupy the potential binding site of CCM2ct by intramolecular interaction, playing a competitive role in undesirable intermolecular interaction. Moreover, CCM2ct intramolecular interaction is intrinsically weak and makes available the potential binding site for appropriate partners. On sensing the upstream signals, the structural element analogous to CCM2-c_{helix} in the partners could occupy the binding site of CCM2ct with much higher binding affinity, resulting in CCM2 acting in a partner-recruitment state and transmitting signals downstream.

Following rational deduction we focused on MEKK3, the first and important partner of CCM2, and mapped the N-terminal isolated helix of MEKK3 as the essential structural element responsible for CCM2ct-MEKK3 recognition. The structure of CCM2ct_s-MEKK3-n_{helix} complex solved in this study provides a precise molecular basis for CCM2ct-MEKK3 recognition. To recruit MEKK3 for signal transduction, CCM2ct_s employs the potential binding site to accept MEKK3-n_{helix} in a manner resembling CCM2ct intramolecular interaction. The specific sequences of MEKK3-n_{helix} introduce more extensive interactions with CCM2ct_s than those of CCM2-c_{helix}, therefore giving rise to greater stability of CCM2ct_s-MEKK3-n_{helix} intermolecular interaction than that of CCM2ct intramolecular interaction. The resulting CCM2-MEKK3 interaction builds a molecular platform for regulating MEKK3 signaling. When the cell is under dangerous conditions such as osmotic stress, CCM2-MEKK3 interaction facilitates the recruitment and activation of a downstream signaling component of MEKK3 signaling, in turn helping the cell to generate a protective response (Uhlik et al., 2003; Zhou et al., 2011). However, during cardiovascular development, increased MEKK3 signaling in endothelial cells is harmful because MEKK3 up-regulates endocardial expression of the KLF2/4 transcription factors and ADAMTS4/5 proteases that degrade cardiac jelly, the important extracellular matrix in the developing heart. Therefore, endothelial CCM2-MEKK3 interaction captures MEKK3 to the efficient CCM signal complex and inhibits MEKK3 activity by an unknown mechanism during normal cardiac development (Zhou et al., 2015). Our findings build an elegant structural framework for understanding CCM2-MEKK3 interaction. The discovered CCM2ct_s-MEKK3-n_{helix} intermolecular interaction raises the possibility that the other parts of CCM2, including the N-terminal part and the released CCM2-c_{helix}, could recruit other partners that regulate MEKK3 signaling in opposite directions.

It is well known that adaptor proteins perform their functions via protein-protein interactions. Two types of protein-protein interactions are characterized by most adaptor proteins, the first of which is homotypic interaction between the interacting modules.

Table 2. Kinetics and Affinity Constants for Wild-Type and Mutant MEKK3nt Proteins Binding to CCM2ct or CCM2ct$_s$

Protein	Association Rate, k_a (M^{-1} s^{-1})	Dissociation Rate, k_d (s^{-1})	Binding Affinity, K_d (M)
MEKK3nt-CCM2ct	2.37×10^4	5.01×10^{-3}	2.11×10^{-7}
MEKK3nt-CCM2ct$_s$	4.90×10^4	1.44×10^{-3}	2.93×10^{-8}
MEKK3nt$_s$-CCM2ct	ND	ND	ND
MEKK3nt$_s$-CCM2ct$_s$	ND	ND	ND
MEKK3nt-E3A-CCM2ct	9.94×10^3	5.15×10^{-3}	5.18×10^{-7}
MEKK3nt-L7D-CCM2ct	ND	ND	ND
MEKK3nt-I10D-CCM2ct	ND	ND	ND
MEKK3nt-L14D-CCM2ct	ND	ND	ND
MEKK3nt-L17D-CCM2ct	ND	ND	ND

ND, not detectable.

The homologous structural modules are present in both the adaptor and its binding partners, and mediate the recruitment of partners by adaptor proteins. Members of the death domain superfamily typically adopt this type of interaction (Park et al., 2007). The other type is sequence motif recognition by the interacting modules, whereby the unique structural modules of adaptor proteins recognize and bind to the specific motifs in its binding partners, giving rise to the tight binding between adaptor and partner proteins. Src-homology 2 (SH2) domain-containing proteins are the most widely known examples of this type of interaction (Songyang et al., 1993). Structural studies on another CCM protein, CCM3, from our and other groups revealed that the N-terminal domain of CCM3 is not only a novel dimerization domain but also a structural module mediating the homotypic interaction with germinal center kinase III (GCKIII) proteins (Ding et al., 2010; Li et al., 2010; Xu et al., 2013; Zhang et al., 2013). These findings classify CCM3 as the adaptor protein featuring the first type of interaction. In this study, our findings on CCM2ct intramolecular interaction and CCM2ct-MEKK3 recognition uncover a harmonin-nt-like structural module CCM2ct$_s$ at the C terminus of CCM2, and define a novel sequence motif L/IxxL/IxxDL/IxxL/I (where x is any residue), which is folded into an isolated amphiphilic helix and specifically recognized by CCM2ct$_s$. Based on these findings, we may categorize CCM2 as the adaptor protein adopting the second type of interaction. Moreover, CCM2 is a multifunctional adaptor protein through its interaction with different partners. The molecular recognition between CCM2ct and MEKK3 provides a sound structural basis for further investigations on whether CCM2 could interact with other partners in a manner similar to that for recognizing MEKK3.

EXPERIMENTAL PROCEDURES

Cloning, Expression, and Purification

CCM2ct (residues 290–444) was constructed, expressed, and purified as previously described (Wang et al., 2012). The same procedure was applied to obtain purified CCM2ct$_s$ (residues 290–376). Both MEKK3nt (residues 1–126) and MEKK3nt$_s$ (residues 42–126) were subcloned into a modified pET-32a(+) vector with a thioredoxin tag, a His$_6$ tag, and a PreScission protease site at the N terminus to facilitate protein folding and purication. *Escherichia coli* BL21 (DE3) cells (Novagen) harboring the recombinant plasmids were grown in LB medium supplemented with 100 μg/ml ampicillin at 310 K until the OD_{600} of the culture reached 0.8. The proteins were then expressed for 3 hr at 310 K after induction with 0.25 mM isopropyl-β-D-thiogalactoside. Cell pellets expressing recombinant MEKK3nt or MEKK3nt$_s$ were harvested and lysed by sonication in lysis buffer (50 mM phosphate saline [pH 8.0], 300 mM sodium chloride, 10 mM imidazole, and 10 mM β-mercaptoethanol). After centrifugation, the soluble proteins were first purified using an Ni-NTA chromatography column (Novagen). The thioredoxin and His$_6$ tags were cleaved with PreScission protease overnight after buffer exchange with lysis buffer. Subsequently, the untagged proteins were again passed through an Ni-NTA chromatography column to deplete the thioredoxin and His$_6$ tags. MEKK3nt and MEKK3nt$_s$ were further purified by size-exclusion chromatography using a Hiload 16/60 Superdex 75 column (GE Healthcare) in buffer (20 mM HEPES [pH 7.5], 150 mM sodium chloride). The CCM2 peptide (residues 417–438) and MEKK3 peptide (residues 1–22) were synthesized by Scilight-Peptide Inc. (Beijing, China). The mutants of MEKK3nt were generated by site-directed mutagenesis using the wild-type vector as the template, and confirmed by DNA sequencing. The expressed and purified procedure for the mutant proteins was the same as that for wild-type proteins.

Crystallization, Data Collection, and Structure Determination

Crystallization and data collection for CCM2ct were as previously described (Wang et al., 2012). CCM2ct$_s$ crystals were grown by the sitting-drop vapor diffusion method at 293 K with 2-μl drops containing 1 μl of protein solution and 1 μl of reservoir solution equilibrated over 80 μl of reservoir solution. The qualified crystals were obtained in the reservoir buffer containing 0.1 M Bis-Tris (pH 6.5), 30% (w/v) polyethylene glycol 550, and 50 mM calcium chloride within 3–4 days, and soaked in a cryoprotecting solution containing reservoir buffer in addition with 10% (v/v) glycerol before being flash-frozen with liquid nitrogen for data collection. Co-crystallization of CCM2ct$_s$ with MEKK3 peptide was performed by the sitting-drop vapor diffusion method at 293 K using the mixture of CCM2ct$_s$ and dissolved MEKK3 peptide at a molar ratio of 1:3. The complex crystals were obtained in the reservoir buffer containing 3.5 M sodium formate (pH 7.0) within 24 hr, and soaked in paraffin oil as a cryoprotecting solution before being flash-frozen with liquid nitrogen for data collection. Diffraction data of CCM2ct$_s$ were collected at the Shanghai Synchrotron Radiation Facility (Shanghai, China), and that of CCM2ct$_s$-MEKK3-n$_{helix}$ complex was collected on a Rigaku FR-E diffraction system using a Rigaku R-Axis IV++ image plate detector at 40 kV and 40 mA. Both data were processed with IMOSFLM and scaled with SCALA from the CCP4 program suite (Dodson et al., 1997).

Phase determination and automatic model building of CCM2ct were performed using the PHENIX program suite (Adams et al., 2010). The rest of the model was manually built with Coot (Emsley et al., 2010). The structures of CCM2ct$_s$ and CCM2ct$_s$-MEKK3-n$_{helix}$ complex were both determined by molecular replacement with PHASER of the CCP4 program suite using the truncated CCM2 structure as a search model. All the structures were refined with PHENIX, and manual modeling was performed between refinement cycles. The statistics of data collection and refinement are summarized in Table 1. The quality of the final model was validated by MolProbity (Chen et al., 2010). Sequence alignments were generated using ClustalW (Chenna et al., 2003), and the sequence alignment figures were produced using ESPript (Robert and Gouet, 2014). All other figures were rendered in PyMOL (http://www.pymol.org).

The atomic coordinates and structure factors for CCM2ct, CCM2ct$_s$ and CCM2ct$_s$-MEKK3-n$_{helix}$ complex (PDB: 4YKC, 4YKD, 4YL6) have been deposited in the PDB of the Research Collaboratory for Structural Bioinformatics, Rutgers University (http://www.rcsb.org/).

ITC Assay

ITC experiments were performed at 298 K using an ITC200 (GE Healthcare). The CCM2 peptide was dissolved in the buffer containing 20 mM HEPES (pH 7.5), 150 mM NaCl, and 5 mM DTT. CCM2ct and CCM2ct$_s$ proteins were exchanged to the same buffer for titration. 3.2 mM CCM2ct$_s$ or 2.1 mM CCM2ct was titrated into the cell containing 0.13 mM or 0.1 mM CCM2 peptide with 2 μl per injection separated by 120 s. A total of 20 injections were delivered. The binding parameters were calculated using Microcal Origin 7.0 software.

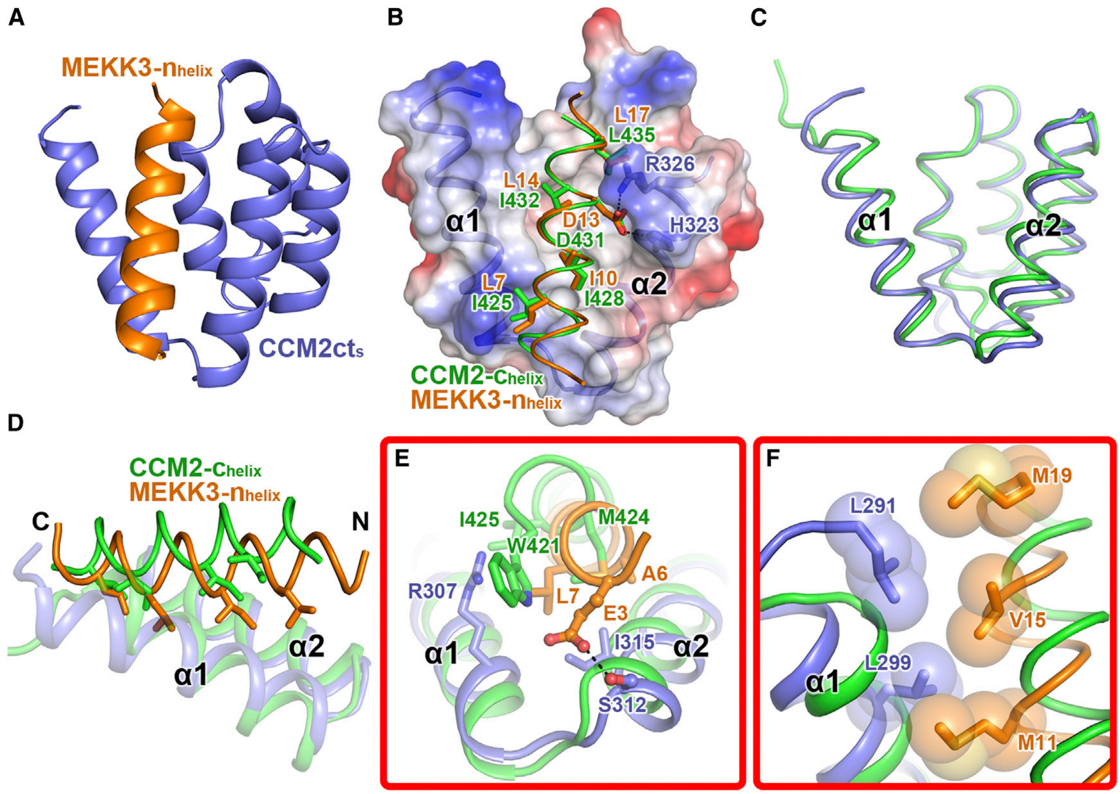

Figure 5. Molecular Recognition between CCM2ct and MEKK3-n$_{helix}$

See also Figure S4.

(A) Overall structure of CCM2ct$_s$-MEKK3-n$_{helix}$ complex in cartoon scheme.

(B) The conserved interactions between the α1/α2 cleft of CCM2ct$_s$ and MEKK3-n$_{helix}$. CCM2ct$_s$ is represented as electrostatic potential surface with the coloration from red to blue for negatively to positively charged regions. CCM2-c$_{helix}$ is superimposed onto MEKK3-n$_{helix}$. The residues involved in conserved interactions are labeled and shown as stick models. Hydrogen bonds are shown as black dashes.

(C) Structural superimposition of CCM2ct$_s$ in complex and its counterpart in CCM2ct.

(D) Structural superimposition of the α1/α2 cleft of CCM2ct$_s$ with its binding target. The conserved hydrophobic residues embedded in the cleft are shown as stick models.

(E and F) Close-up views of the specific interactions between both MEKK3-n$_{helix}$ terminus and the α1/α2 cleft of CCM2ct$_s$.

Analytical Ultracentrifugation

Sedimentation velocity measurement was performed on CCM2ct. The sample was loaded at the concentration yielding initial A_{280} values of 0.8. Ultracentrifugation was performed at 298 K in buffer containing 20 mM HEPES (pH 7.5) and 150 mM NaCl using an Optima XL-I analytical ultracentrifuge (Beckman Instruments, Palo Alto, CA) with an An50-Ti rotor. The sample was run for 8 hr at a rotor speed of 60,000 rpm. The data were analyzed according to the concentration (M) method using the SEDFIT software package.

Pull-down Assay

The Ni-NTA beads pre-equilibrated with lysis buffer were coated with excess purified CCM2ct-His$_6$ or CCM2ct$_s$-His$_6$ proteins and incubated with equimolar MEKK3nt or MEKK3nt$_s$ for 30 min at 277 K. The beads were then washed three times using lysis buffer, and the unbound proteins collected. The proteins bound on the beads were eluted by lysis buffer supplemented with 300 mM imidazole. All the protein samples including the inputs were analyzed by SDS-PAGE.

SPR Kinetic Assay

SPR experiments were carried out at 298 K using a Biacore 3000 optical biosensor equipped with a CM5 sensor chip. A running buffer containing 20 mM HEPES (pH 7.5), 150 mM NaCl, and 0.005% (v/v) Tween-20 was used for all measurements. A total of 3,200 response units (RU) of CCM2ct and 1,075 RU of CCM2ct$_s$ were immobilized on the chip prior to blockade with ethanolamine in reaction to the MEKK3 peptide. 270 RU of CCM2ct and 137 RU of CCM2ct$_s$ were immobilized on the chip in reaction to wild-type MEKK3nt or MEKK3nt$_s$ in addition to MEKK3nt mutants. The samples of MEKK3 peptide, MEKK3nt, MEKK3nt$_s$ and MEKK3nt mutants were injected at different concentrations with a flow rate of 40 μl/min. When the data collection for each cycle was complete, the sensor surface was regenerated with 5 mM NaOH. Sensorgrams were fit globally with Biacore T100 evaluation software using a steady-state affinity model for CCM2ct or CCM2ct$_s$ interactions with MEKK3 peptide and a 1:1 Langmuir binding model for those with wild-type MEKK3nt or MEKK3nt mutants.

SUPPLEMENTAL INFORMATION

Supplemental Information includes four figures and can be found with this article online at http://dx.doi.org/10.1016/j.str.2015.04.003.

ACKNOWLEDGMENTS

The authors thank Yi Han and Yuanyuan Chen (Institute of Biophysics, Chinese Academy of Sciences) for their assistance with in-house data collection, ITC, and Biacore analysis, and the staff at beamline NW12A of the Photon Factory (2011G044, KEK, Japan) and at beamline BL17U of Shanghai Synchrotron

Radiation Facility (Shanghai, China) for technical assistance during data collection. This work was funded by the Chinese Ministry of Science and Technology 973 program (grants 2011CB910304 and 2011CB911103), the Strategic Priority Research Program of the Chinese Academy of Sciences (grant XDB08020200), the Key Program of the Chinese Academy of Sciences (KJZD-EW-L02), and the National Natural Science Foundation of China (grant 31100535).

Received: December 8, 2014
Revised: March 16, 2015
Accepted: April 2, 2015
Published: May 14, 2015

REFERENCES

Adams, P.D., Afonine, P.V., Bunkoczi, G., Chen, V.B., Davis, I.W., Echols, N., Headd, J.J., Hung, L.W., Kapral, G.J., Grosse-Kunstleve, R.W., et al. (2010). PHENIX: a comprehensive Python-based system for macromolecular structure solution. Acta Crystallogr. D Biol. Crystallogr. *66*, 213–221.

Bhattacharyya, R.P., Remenyi, A., Yeh, B.J., and Lim, W.A. (2006). Domains, motifs, and scaffolds: the role of modular interactions in the evolution and wiring of cell signaling circuits. Annu. Rev. Biochem. *75*, 655–680.

Borikova, A.L., Dibble, C.F., Sciaky, N., Welch, C.M., Abell, A.N., Bencharit, S., and Johnson, G.L. (2010). Rho kinase inhibition rescues the endothelial cell cerebral cavernous malformation phenotype. J. Biol. Chem. *285*, 11760–11764.

Chen, V.B., Arendall, W.B., 3rd, Headd, J.J., Keedy, D.A., Immormino, R.M., Kapral, G.J., Murray, L.W., Richardson, J.S., and Richardson, D.C. (2010). MolProbity: all-atom structure validation for macromolecular crystallography. Acta Crystallogr. D Biol. Crystallogr. *66*, 12–21.

Chenna, R., Sugawara, H., Koike, T., Lopez, R., Gibson, T.J., Higgins, D.G., and Thompson, J.D. (2003). Multiple sequence alignment with the Clustal series of programs. Nucleic Acids Res. *31*, 3497–3500.

Costa, B., Kean, M.J., Ast, V., Knight, J.D., Mett, A., Levy, Z., Ceccarelli, D.F., Badillo, B.G., Eils, R., Konig, R., et al. (2012). STK25 protein mediates TrkA and CCM2 protein-dependent death in pediatric tumor cells of neural origin. J. Biol. Chem. *287*, 29285–29289.

Crose, L.E., Hilder, T.L., Sciaky, N., and Johnson, G.L. (2009). Cerebral cavernous malformation 2 protein promotes smad ubiquitin regulatory factor 1-mediated RhoA degradation in endothelial cells. J. Biol. Chem. *284*, 13301–13305.

Denier, C., Goutagny, S., Labauge, P., Krivosic, V., Arnoult, M., Cousin, A., Benabid, A.L., Comoy, J., Frerebeau, P., Gilbert, B., et al. (2004). Mutations within the MGC4607 gene cause cerebral cavernous malformations. Am. J. Hum. Genet. *74*, 326–337.

Ding, J., Wang, X., Li, D.F., Hu, Y., Zhang, Y., and Wang, D.C. (2010). Crystal structure of human programmed cell death 10 complexed with inositol-(1,3,4,5)-tetrakisphosphate: a novel adaptor protein involved in human cerebral cavernous malformation. Biochem. Biophys. Res. Commun. *399*, 587–592.

Dodson, E.J., Winn, M., and Ralph, A. (1997). Collaborative Computational Project, number 4: providing programs for protein crystallography. Methods Enzymol. *277*, 620–633.

Emsley, P., Lohkamp, B., Scott, W.G., and Cowtan, K. (2010). Features and development of Coot. Acta Crystallogr. D Biol. Crystallogr. *66*, 486–501.

Faurobert, E., and Albiges-Rizo, C. (2010). Recent insights into cerebral cavernous malformations: a complex jigsaw puzzle under construction. FEBS J. *277*, 1084–1096.

Fisher, O.S., Zhang, R., Li, X., Murphy, J.W., Demeler, B., and Boggon, T.J. (2013). Structural studies of cerebral cavernous malformations 2 (CCM2) reveal a folded helical domain at its C-terminus. FEBS Lett. *587*, 272–277.

Flynn, D.C. (2001). Adaptor proteins. Oncogene *20*, 6270–6272.

Good, M.C., Zalatan, J.G., and Lim, W.A. (2011). Scaffold proteins: hubs for controlling the flow of cellular information. Science *332*, 680–686.

Harel, L., Costa, B., Tcherpakov, M., Zapatka, M., Oberthuer, A., Hansford, L.M., Vojvodic, M., Levy, Z., Chen, Z.Y., Lee, F.S., et al. (2009). CCM2 mediates death signaling by the TrkA receptor tyrosine kinase. Neuron *63*, 585–591.

Hilder, T.L., Malone, M.H., Bencharit, S., Colicelli, J., Haystead, T.A., Johnson, G.L., and Wu, C.C. (2007). Proteomic identification of the cerebral cavernous malformation signaling complex. J. Proteome Res. *6*, 4343–4355.

Holm, L., and Sander, C. (1995). Dali: a network tool for protein structure comparison. Trends Biochem. Sci. *20*, 478–480.

Kleaveland, B., Zheng, X., Liu, J.J., Blum, Y., Tung, J.J., Zou, Z., Sweeney, S.M., Chen, M., Guo, L., Lu, M.M., et al. (2009). Regulation of cardiovascular development and integrity by the heart of glass-cerebral cavernous malformation protein pathway. Nat. Med. *15*, 169–176.

Labauge, P., Denier, C., Bergametti, F., and Tournier-Lasserve, E. (2007). Genetics of cavernous angiomas. Lancet Neurol. *6*, 237–244.

Li, X., Zhang, R., Zhang, H., He, Y., Ji, W., Min, W., and Boggon, T.J. (2010). Crystal structure of CCM3, a cerebral cavernous malformation protein critical for vascular integrity. J. Biol. Chem. *285*, 24099–24107.

Liquori, C.L., Berg, M.J., Siegel, A.M., Huang, E., Zawistowski, J.S., Stoffer, T., Verlaan, D., Balogun, F., Hughes, L., Leedom, T.P., et al. (2003). Mutations in a gene encoding a novel protein containing a phosphotyrosine-binding domain cause type 2 cerebral cavernous malformations. Am. J. Hum. Genet. *73*, 1459–1464.

Liquori, C.L., Berg, M.J., Squitieri, F., Leedom, T.P., Ptacek, L., Johnson, E.W., and Marchuk, D.A. (2007). Deletions in CCM2 are a common cause of cerebral cavernous malformations. Am. J. Hum. Genet. *80*, 69–75.

Pan, L., Yan, J., Wu, L., and Zhang, M. (2009). Assembling stable hair cell tip link complex via multidentate interactions between harmonin and cadherin 23. Proc. Natl. Acad. Sci. USA *106*, 5575–5580.

Pan, C.Q., Sudol, M., Sheetz, M., and Low, B.C. (2012). Modularity and functional plasticity of scaffold proteins as p(l)acemakers in cell signaling. Cell Signal. *24*, 2143–2165.

Park, H.H., Lo, Y.C., Lin, S.C., Wang, L., Yang, J.K., and Wu, H. (2007). The death domain superfamily in intracellular signaling of apoptosis and inflammation. Annu. Rev. Immunol. *25*, 561–586.

Robert, X., and Gouet, P. (2014). Deciphering key features in protein structures with the new ENDscript server. Nucleic Acids Res. *42*, W320–W324.

Rosen, J.N., Sogah, V.M., Ye, L.Y., and Mably, J.D. (2013). ccm2-like is required for cardiovascular development as a novel component of the Heg-CCM pathway. Dev. Biol. *376*, 74–85.

Songyang, Z., Shoelson, S.E., Chaudhuri, M., Gish, G., Pawson, T., Haser, W.G., King, F., Roberts, T., Ratnofsky, S., Lechleider, R.J., et al. (1993). SH2 domains recognize specific phosphopeptide sequences. Cell *72*, 767–778.

Stockton, R.A., Shenkar, R., Awad, I.A., and Ginsberg, M.H. (2010). Cerebral cavernous malformations proteins inhibit Rho kinase to stabilize vascular integrity. J. Exp. Med. *207*, 881–896.

Uhlik, M.T., Abell, A.N., Johnson, N.L., Sun, W., Cuevas, B.D., Lobel-Rice, K.E., Horne, E.A., Dell'Acqua, M.L., and Johnson, G.L. (2003). Rac-MEKK3-MKK3 scaffolding for p38 MAPK activation during hyperosmotic shock. Nat. Cell Biol. *5*, 1104–1110.

Voss, K., Stahl, S., Schleider, E., Ullrich, S., Nickel, J., Mueller, T.D., and Felbor, U. (2007). CCM3 interacts with CCM2 indicating common pathogenesis for cerebral cavernous malformations. Neurogenetics *8*, 249–256.

Wang, X., Ding, J., and Wang, D. (2012). Crystallization and preliminary X-ray analysis of the C-terminal domain of CCM2, part of a novel adaptor protein involved in cerebral cavernous malformations. Acta Crystallogr. Sect. F Struct. Biol. Cryst. Commun. *68*, 683–686.

Whitehead, K.J., Chan, A.C., Navankasattusas, S., Koh, W., London, N.R., Ling, J., Mayo, A.H., Drakos, S.G., Jones, C.A., Zhu, W., et al. (2009). The cerebral cavernous malformation signaling pathway promotes vascular integrity via Rho GTPases. Nat. Med. *15*, 177–184.

Wu, C., Haynes, E.M., Asokan, S.B., Simon, J.M., Sharpless, N.E., Baldwin, A.S., Davis, I.J., Johnson, G.L., and Bear, J.E. (2013). Loss of Arp2/3 induces an NF-kappaB-dependent, nonautonomous effect on chemotactic signaling. J. Cell Biol. *203*, 907–916.

Xu, X., Wang, X., Zhang, Y., Wang, D.C., and Ding, J. (2013). Structural basis for the unique heterodimeric assembly between cerebral cavernous malformation 3 and germinal center kinase III. Structure *21*, 1059–1066.

Zawistowski, J.S., Stalheim, L., Uhlik, M.T., Abell, A.N., Ancrile, B.B., Johnson, G.L., and Marchuk, D.A. (2005). CCM1 and CCM2 protein interactions in cell signaling: implications for cerebral cavernous malformations pathogenesis. Hum. Mol. Genet. *14*, 2521–2531.

Zhang, M., Dong, L., Shi, Z., Jiao, S., Zhang, Z., Zhang, W., Liu, G., Chen, C., Feng, M., Hao, Q., et al. (2013). Structural mechanism of CCM3 heterodimerization with GCKIII kinases. Structure *21*, 680–688.

Zheng, X., Xu, C., Smith, A.O., Stratman, A.N., Zou, Z., Kleaveland, B., Yuan, L., Didiku, C., Sen, A., Liu, X., et al. (2012). Dynamic regulation of the cerebral cavernous malformation pathway controls vascular stability and growth. Dev. Cell *23*, 342–355.

Zhou, X., Izumi, Y., Burg, M.B., and Ferraris, J.D. (2011). Rac1/osmosensing scaffold for MEKK3 contributes via phospholipase C-gamma1 to activation of the osmoprotective transcription factor NFAT5. Proc. Natl. Acad. Sci. USA *108*, 12155–12160.

Zhou, Z., Rawnsley, D.R., Goddard, L.M., Pan, W., Cao, X.J., Jakus, Z., Zheng, H., Yang, J., Arthur, J.S., Whitehead, K.J., et al. (2015). The cerebral cavernous malformation pathway controls cardiac development via regulation of endocardial MEKK3 signaling and KLF expression. Dev. Cell *32*, 168–180.

